

UC Irvine

UC Irvine Previously Published Works

Title

Synthetic Sphingolipids with 1,2-Pyridazine Appendages Improve Antiproliferative Activity in Human Cancer Cell Lines.

Permalink

<https://escholarship.org/uc/item/5v3395xc>

Journal

ACS Medicinal Chemistry Letters, 11(5)

ISSN

1948-5875

Authors

Bachollet, Sylvestre

Vece, Vito

McCracken, Alison

et al.

Publication Date

2020-05-14

DOI

10.1021/acsmchemlett.9b00553

Peer reviewed

Synthetic Sphingolipids with 1,2-Pyridazine Appendages Improve Antiproliferative Activity in Human Cancer Cell Lines

Sylvestre P. J. T. Bachollet,[§] Vito Vece,[§] Alison N. McCracken,[§] Brendan T. Finicle, Elizabeth Selwan, Nadine Ben Romdhane, Amogha Dahal, Cuauhtemoc Ramirez, Aimee L. Edinger,* and Stephen Hanessian*

Cite This: *ACS Med. Chem. Lett.* 2020, 11, 686–690

Read Online

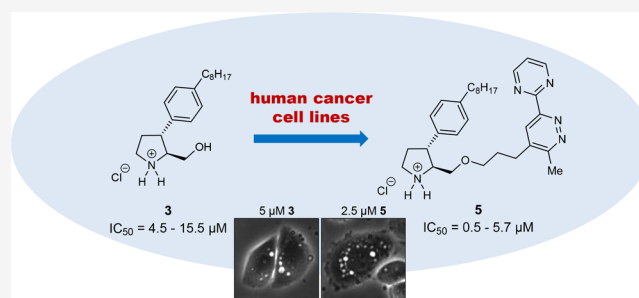
ACCESS |

Metrics & More

Article Recommendations

Supporting Information

ABSTRACT: A synthetic sphingolipid related to a ring-constrained hydroxymethyl pyrrolidine analog of FTY720 that was known to starve cancer cells to death was chemically modified to include a series of alkoxy-tethered 3,6-substituted 1,2-pyridazines. These derivatives exhibited excellent antiproliferative activity against eight human cancer cell lines from four different cancer types. A 2.5- to 9-fold reduction in IC_{50} in these cell lines was observed relative to the lead compound, which lacked the appended heterocycle.



KEYWORDS: sphingolipid, anticancer, KRAS mutant cancer, nutrient transporter, vacuolation

Sphingolipids are a family of evolutionarily conserved natural compounds that play essential roles in the life cycle of cells.^{1–3} A subset of sphingolipids, such as phytosphingosine, slows cell growth, induces differentiation, and triggers cell death (Figure 1, compound 1). As part of the adaptive response to stress, compound 1 down-regulates nutrient transporters in yeast, reducing access to amino acids and uracil and inducing a stress-resistant quiescent state.⁴ Although mammalian cells do not produce phytosphingosine, the sphingolipid ceramide, a 4,5-unsaturated congener, has a

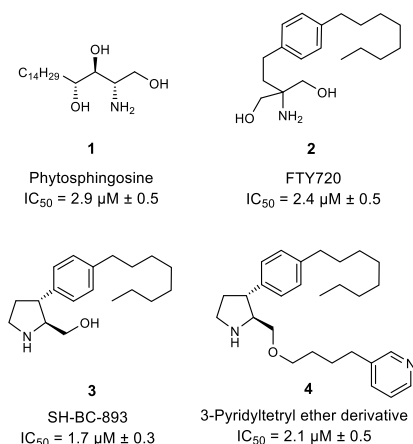


Figure 1. Structures of antiproliferative synthetic compounds related to sphingosine (1–3) and 3-pyridyl-appended analog of 3 (4). IC_{50} in FLS.12 cells is shown.

similar effect on mammalian nutrient transporters for amino acids and glucose.^{5,6} Whereas limiting nutrient access produces adaptive quiescence in normal cells, the oncogenic mutations in cancer cells constitutively drive growth, rendering transformed cells hypersensitive to interruptions in the nutrient supply.^{7,8} Indeed, many standard-of-care chemotherapies target biosynthetic pathways, and cancer therapies that disrupt anabolism are under development.⁹

Our group has developed synthetic sphingolipid analogs that recapitulate the ability of natural sphingolipids to starve cancer cells to death.^{8,10,11} Being cognizant of the challenges associated with using a natural molecule like ceramide as a drug (e.g., poor solubility and rapid metabolism), we turned to the synthetic sphingolipid FTY720 (Fingolimod). At higher doses than is required to affect sphingosine-1-phosphate receptors, FTY720 limits nutrient access and starves cancer cells to death.^{10,11} In addition to reducing the levels of glucose and amino acid transporters on the cell surface, FTY720 also disrupts lysosomal fusion reactions.^{6,11} This disruption, visualized as cellular vacuolation, additionally limits access to nutrients acquired from the digestion of low-density lipoprotein (LDL) particles, autophagosomes, and macrophages.^{8,11,12} Despite its activity in multiple preclinical

Special Issue: In Memory of Maurizio Botta: His Vision of Medicinal Chemistry

Received: November 26, 2019

Accepted: February 12, 2020

Published: February 12, 2020



cancer models, FTY720 cannot be repurposed as a cancer therapy because the phosphorylated form triggers severe bradycardia at the doses required to kill neoplastic cells.^{10,13–16}

We have reported that the synthetic sphingolipid compound 3 (SH-BC-893), a constrained variant of FTY720, exhibits favorable activity as an anticancer agent without the negative cardiovascular effects associated with FTY720.^{11,16,17} Like FTY720, compound 3 triggers the internalization of nutrient transporters and blocks lysosome-dependent nutrient generation pathways.^{6,11} Compound 3 significantly inhibits the growth of colon cancer xenografts and autochthonous prostate tumors in a genetically modified mouse model.¹¹ Importantly, compound 3 affects both normal and transformed cells but is toxic only to tumor cells. Compound 3 did not disrupt normal organ function, cause bone marrow suppression, or negatively affect the rapidly proliferating cells of the gut, even upon chronic administration of the anticancer dose.¹¹ Thus compound 3 is both efficacious and well-tolerated, at least in mice.

These results showed the benefits and feasibility of concurrently blocking parallel nutrient access pathways that are essential for proliferating cancer cells. Because compound 3 simultaneously reduces access to glucose, amino acids, and cholesterol,^{6,11} it is expected to be effective even against heterogeneous tumors and may be less susceptible to the rapid development of resistance observed with many targeted therapies. Whereas it has many activities desirable in an anticancer agent, the low micromolar potency exhibited by compound 3 might be improved by additional derivatization.

In previous studies, we delineated the structural and functional features in compound 3 that contributed to cytotoxicity.¹⁸ The phenyloctyl appendage was found to be susceptible to changes in the length of the octyl chain and the presence of polar groups, except at the benzylic position. The extension of the hydroxymethyl group to include alkyl ethers containing heterocyclic moieties such as a 3-pyridyl-appended variant (Figure 1, compound 4) was tolerated.¹⁹ We were intrigued that the inclusion of a 3-pyridyl unit as an appendage did not negatively affect the cytotoxicity of the original compound 3.

In an effort to further explore the effects of heteroaromatic appendages, we turned our attention to 1,2-pyridazine as a heterocycle that has found many applications as a versatile biological probe.^{20–26}

In view of the presence of an extended (or folded) hydrophobic chain and an appended aromatic heterocycle anchored on a basic pyrrolidine core, it is possible to envisage certain hypothetical interactions with a biological target, as exemplified by structure A in Figure 2. The synthetic protocol we chose allowed for the generation of a series of 3,6-disubstituted 1,2-pyridazines appended to the lead compound 3 via a two- to three-carbon chain ether linker. We further surmised that the relatively flexible single bonds of the 3,6-substituents would adopt conformationally favorable spatial orientations. Although we have previously established that compound 3 activates PP2A,^{6,11,27} we do not yet know the mechanism by which this occurs.

With this premise in mind, we developed a strategy that engaged the terminal olefinic ether appendages of 3 with 3,6-disubstituted 1,2,4,5-tetrazines in an inverse electron demand Diels–Alder reaction to give the corresponding 3,6-disubstituted 1,2-pyridazines²⁸ as a 1:1 mixtures of 4,5-regioisomers (Scheme 1). Cytotoxicity, nutrient transporter down-regula-

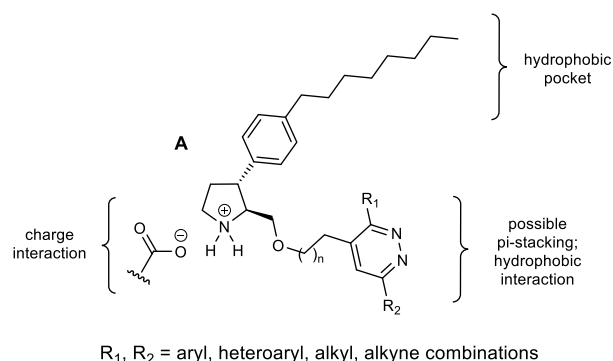
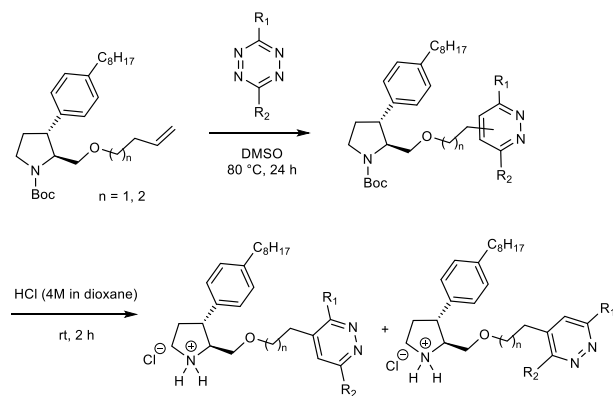


Figure 2. Hypothetical interactions of compound 3/pyridazine-ether-appended constructs (A). Only one regioisomer is shown in the 1,2-pyridazine ring.

Scheme 1. General Scheme for the Synthesis of the 3,6-Disubstituted 1,2-Pyridazine Derivatives as 1:1 Mixtures of 4,5-Regioisomers



tion, and vacuolation induced by the products were then measured in FL5.12 murine hematopoietic cells, a cell line that grows in suspension and is therefore well-suited to flow-cytometry-based assays for transporter loss. Cytotoxicity was also evaluated in a panel of human cancer cell lines for compounds of interest. (See Figure 3 and Supplementary Table 3.)

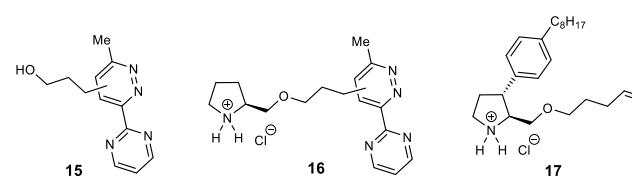


Figure 3. 1,2-Pyridazine derivatives and a 1-butenyl ether of 3 for the comparison of biological activities.

Table 1 lists the activity of a variety of analogs. We were pleased that a 1:1 mixture of regioisomers of compound 5 having methyl and 1,3-pyrimidine substituents on the 1,2-pyridazine core surpassed the activity of the parent 3, reaching the high nanomolar threshold for the first time in this series. In fact, the two regioisomers 5a and 5b could be separated by chromatography and exhibited IC₅₀ values of 0.5 and 0.7 μM, respectively. Despite its increased potency in cytotoxicity assays, compound 5 did not down-regulate amino acid transporters or vacuolate FL5.12 cells at the concentrations that killed cells; 10 μM was required to observe these effects.

Table 1. Cytotoxicity of the Synthetic Pyridazine Derivatives in FL5.12 Cells^a

Comp.	n	R ₁	R ₂	IC ₅₀
5a	2	CH ₃		0.5 μM ± 0.2
5b	2		CH ₃	0.7 μM ± 0.4
6	1	CH ₃		1.7 μM ± 0.4
7	2	CH ₃		1.6 μM ± 0.5
8	2	CH ₃		1.3 μM ± 0.4
9	2	CH ₃		2.8 μM ± 0.4
10	2	CH ₃		3.3 μM ± 0.3
11	2	CH ₃	CH ₃	1.3 μM ± 0.3
12	2			1.8 μM ± 0.6
13	2			1.4 μM ± 0.3
14	2			0.9 μM ± 0.1

^aValues represent mean ± SD. Compounds 6–10 are 1:1 mixtures of 4- and 5-substituted isomers. The IC₅₀ value for a 1:1 mixture of 5a and 5b was 0.9 μM ± 0.1.

(See Supplementary Table 1.) However, it is of particular interest that compound 5 efficiently triggered transporter loss and vacuolation in MDA-MB-468 breast cancer cells. (See Supplementary Figure 1.) These discrepancies may arise from differences in the subunit composition of PP2A heterotrimers, the post-translational modification of PP2A subunits, or the subcellular localization of PP2A in these various cell lines. In summary, given its ability to fully phenocopy the PP2A-dependent effects of compound 3 in cancer cells, it is likely that compound 5 shares the PP2A-related target of compound 3. On the contrary, the ability of compound 5 to efficiently kill FL5.12 cells without inducing transporter loss or vacuolation suggests for the first time that there may be another target of this chemical series that makes an important, and partially redundant, contribution to its anticancer effects. On-going target deconvolution studies are expected to provide insight into these points.

Although there was a clear preference for a methyl and a pyrimidine group attached to the 3- and 6-positions of the

pyridazine in analogs 5a and 5b compared with all of the others in Table 1, the differences in IC₅₀ values varied by only a factor of 5 for the least active compound (10). Decreasing the number of carbons in the linker from three to two, as in compound 6, resulted in a three-fold increase in IC₅₀ compared with 5a or 5b without affecting its ability to down-regulate nutrient transporters or to vacuolate (Supplemental Table 1). The relatively unremarkable structure–activity relationship (SAR) within this limited series of derivatives suggests that the central pyridazine core with a 3,6-substitution pattern of small or large groups such as methyl and aryl or heteroaryl, respectively, is well-tolerated. Importantly, compounds consisting of only the pyridazine moiety (15) and compound 6 devoid of the phenyloctyl chain (16) were inactive (Figure 3, Table 2, Supplementary Table

Table 2. Cytotoxicity of Pyridazine Control Compounds in FL5.12 Cells^a

comp.	IC ₅₀
3	1.7 ± 0.3
15	>40
16	>40
17	2.9 ± 0.2

^aValues represent mean ± SD.

2). However, compound 17 with the ether linker but without the pyridazine minimally affected the cytotoxicity of 3. Clearly, adding the pyridazine moiety to the linker in compound 17, in particular, exemplified by compounds 5a and 5b (or the 1:1 mixture of regioisomers), improves the activity of the current lead compound 3.

Encouraged by the improved cytotoxicity of compound 5 in FL5.12 cells, we conducted additional tests to evaluate its antineoplastic potential compared with the parent compound 3 in eight human cancer cell lines from four different cancer types. We were pleased to find that the superior activity of compound 5 was indeed reproduced. In fact, as a 1:1 mixture of isomers, compound 5 was consistently more potent than the parent compound 3, with IC₅₀ values from ~2.5 to 9 times lower than those of 3 (Figure 4), substantiating the role of the pyridazine core unit as a preferred heterocyclic appendage. We further confirmed that, as in FL5.12, the presence of a pyridine (compound 4) is not sufficient for increased potency and that the nature of the substituents on the pyridazine plays a role in activity (compound 5 vs 9) in HCT116 colon cancer cells. (See Supplementary Table 3.) Finally, it is worth noting that in three KRAS mutant cancer cell lines, compound 5 is between 7 and >20 times more potent than the published small molecule activator of PP2A (SMAP), which is reported to inhibit the proliferation of KRAS mutant lung cancers.²⁹ (See Supplementary Figure 2.) Even the parent compound 3 is at least two times more potent than SMAP in these cell lines.

In conclusion, we have established a novel series of synthetic sphingolipids related to a lead compound 3, with appended 1,2-pyridazine units bearing substituents at the 3,6-positions via a three-carbon ether linker. Whereas a combination of substituents were tolerated in maintaining cytotoxicity against FL5.12 cells, the inclusion of a methyl and a pyrimidinyl group proved to be particularly beneficial in rendering high nanomolar cytotoxicity for the first time in this series. The extension of these activities to selected human cancer cell lines at the nanomolar level augurs well for the development of well-

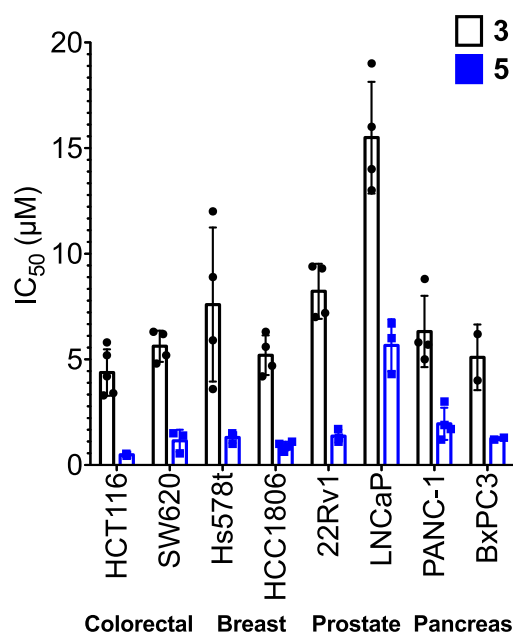


Figure 4. Compound 5 has a lower IC₅₀ than compound 3 across human cancer cell lines.

tolerated cancer therapies that target multiple nutrient import pathways to starve cancer cells to death. Studies are in progress to identify the specific cellular targets of these structurally related natural and synthetic sphingolipids. The 3,6-disubstituted 1,2-pyridazines developed here will be invaluable in these efforts to pinpoint the protein targets of the antiproliferative compound 3 and its analogs.

■ ASSOCIATED CONTENT

Supporting Information

The Supporting Information is available free of charge at <https://pubs.acs.org/doi/10.1021/acsmchemlett.9b00553>.

Biological and chemical methods and chemical experimental procedures (PDF)

■ AUTHOR INFORMATION

Corresponding Authors

Aimee L. Edinger – Department of Developmental and Cell Biology, University of California, Irvine, California 92697-2300, United States; Email: aedinger@uci.edu

Stephen Hanessian – Department of Chemistry, Université de Montréal, Montréal, Quebec H3C 3J7, Canada; orcid.org/0000-0003-3582-6972; Email: stephen.hanessian@umontreal.ca

Authors

Sylvestre P. J. T. Bachollet – Department of Chemistry, Université de Montréal, Montréal, Quebec H3C 3J7, Canada

Vito Vece – Department of Chemistry, Université de Montréal, Montréal, Quebec H3C 3J7, Canada

Alison N. McCracken – Department of Developmental and Cell Biology, University of California, Irvine, California 92697-2300, United States

Brendan T. Finicle – Department of Developmental and Cell Biology, University of California, Irvine, California 92697-2300, United States

Elizabeth Selwan – Department of Developmental and Cell Biology, University of California, Irvine, California 92697-2300, United States; orcid.org/0000-0002-0579-3930

Nadine Ben Romdhane – Department of Developmental and Cell Biology, University of California, Irvine, California 92697-2300, United States

Amogha Dahal – Department of Developmental and Cell Biology, University of California, Irvine, California 92697-2300, United States

Cuauhtemoc Ramirez – Department of Developmental and Cell Biology, University of California, Irvine, California 92697-2300, United States

Complete contact information is available at:

<https://pubs.acs.org/doi/10.1021/acsmchemlett.9b00553>

Author Contributions

[§]S.P.J.T.B., V.V., and A.N.M. contributed equally.

Notes

The authors declare the following competing financial interest(s): S.H. and A.L.E. hold equity in Siegel Pharmaceuticals which is developing compounds in this series for use in cancer and other diseases. S.H. is paid consultant for Siegel, A.L.E. is on the Boards of Directors. Other authors declare no competing financial interest.

■ ACKNOWLEDGMENTS

The Montreal group thanks NSERC for financial assistance. Funding for A.L.E. was provided through a grant from the Chao Family Comprehensive Cancer Center Anti-Cancer Challenge.

■ REFERENCES

- Hannun, Y. A.; Obeid, L. M. Sphingolipids and their metabolism in physiology and disease. *Nat. Rev. Mol. Cell Biol.* **2018**, *19*, 175–191.
- Ogretmen, B. Sphingolipid metabolism in cancer signalling and therapy. *Nat. Rev. Cancer* **2018**, *18*, 33–50.
- Liao, J. Y.; Tao, J. H.; Lin, G. Q.; Liu, D. G. Chemistry and biology of sphingolipids. *Tetrahedron* **2005**, *61*, 4715–4733.
- Welsch, C. A.; Roth, L. W.; Goetschy, J. F.; Movva, N. R. Genetic, biochemical, and transcriptional responses of *Saccharomyces cerevisiae* to the novel immunomodulator FTY720 largely mimic those of the natural sphingolipid phytosphingosine. *J. Biol. Chem.* **2004**, *279*, 36720–36731.
- Guenther, G. G.; Peralta, E. R.; Rosales, K. R.; Wong, S. Y.; Siskind, L. J.; Edinger, A. L. Ceramide starves cells to death by downregulating nutrient transporter proteins. *Proc. Natl. Acad. Sci. U. S. A.* **2008**, *105*, 17402–17407.
- Finicle, B. T.; Ramirez, M. U.; Liu, G.; Selwan, E. M.; McCracken, A. N.; Yu, J.; Joo, Y.; Nguyen, J.; Ou, K.; Roy, S. G.; Mendoza, V. D.; Corrales, D. V.; Edinger, A. L. Sphingolipids inhibit endosomal recycling of nutrient transporters by inactivating ARF6. *J. Cell Sci.* **2018**, *131*, jcs213314.
- McCracken, A. N.; Edinger, A. L. Nutrient transporters: the Achilles' heel of anabolism. *Trends Endocrinol. Metab.* **2013**, *24*, 200–208.
- Selwan, E. M.; Finicle, B. T.; Kim, S. M.; Edinger, A. L. Attacking the supply wagons to starve cancer cells to death. *FEBS Lett.* **2016**, *590*, 885–907.
- Vander Heiden, M. G.; DeBerardinis, R. J. Understanding the Intersections between Metabolism and Cancer Biology. *Cell* **2017**, *168*, 657–669.
- Romero Rosales, K.; Singh, G.; Wu, K.; Chen, J.; Janes, M. R.; Lilly, M. B.; Peralta, E. R.; Siskind, L. J.; Bennett, M. J.; Fruman, D. A.; Edinger, A. L. Sphingolipid-based drugs selectively kill cancer cells

by down-regulating nutrient transporter proteins. *Biochem. J.* **2011**, *439*, 299–311.

(11) Kim, S. M.; Roy, S. G.; Chen, B.; Nguyen, T. M.; McMonigle, R. J.; McCracken, A. N.; Zhang, Y.; Kofuji, S.; Hou, J.; Selwan, E.; Finicle, B. T.; Nguyen, T. T.; Ravi, A.; Ramirez, M. U.; Wiher, T.; Guenther, G. G.; Kono, M.; Sasaki, A. T.; Weisman, L. S.; Potma, E. O.; Tromberg, B. J.; Edwards, R. A.; Hanessian, S.; Edinger, A. L. Targeting cancer metabolism by simultaneously disrupting parallel nutrient access pathways. *J. Clin. Invest.* **2016**, *126*, 4088–4102.

(12) Finicle, B. T.; Jayashankar, V.; Edinger, A. L. Nutrient scavenging in cancer. *Nat. Rev. Cancer* **2018**, *18*, 619–633.

(13) Neviani, P.; Santhanam, R.; Oaks, J. J.; Eiring, A. M.; Notari, M.; Blaser, B. W.; Liu, S.; Trotta, R.; Muthusamy, N.; Gambacorti-Passerini, C.; Druker, B. J.; Cortes, J.; Marcucci, G.; Chen, C. S.; Verrills, N. M.; Roy, D. C.; Caligiuri, M. A.; Bloomfield, C. D.; Byrd, J. C.; Perrotti, D. FTY720, a new alternative for treating blast crisis chronic myelogenous leukemia and Philadelphia chromosome-positive acute lymphocytic leukemia. *J. Clin. Invest.* **2007**, *117*, 2408–2421.

(14) Azuma, H.; Takahara, S.; Horie, S.; Muto, S.; Otsuki, Y.; Katsuoka, Y. Induction of apoptosis in human bladder cancer cells in vitro and in vivo caused by FTY720 treatment. *J. Urol.* **2003**, *169*, 2372–2377.

(15) Azuma, H.; Takahara, S.; Ichimaru, N.; Wang, J. D.; Itoh, Y.; Otsuki, Y.; Morimoto, J.; Fukui, R.; Hoshiga, M.; Ishihara, T.; Nonomura, N.; Suzuki, S.; Okuyama, A.; Katsuoka, Y. Marked prevention of tumor growth and metastasis by a novel immunosuppressive agent, FTY720, in mouse breast cancer models. *Cancer Res.* **2002**, *62*, 1410–1419.

(16) Camm, J.; Hla, T.; Bakshi, R.; Brinkmann, V. Cardiac and vascular effects of fingolimod: Mechanistic basis and clinical implications. *Am. Heart J.* **2014**, *168*, 632–644.

(17) Chen, B.; Roy, S. G.; McMonigle, R. J.; Keebaugh, A.; McCracken, A. N.; Selwan, E.; Fransson, R.; Fallegger, D.; Huwiler, A.; Kleinman, M. T.; Edinger, A. L.; Hanessian, S. Azacyclic FTY720 Analogues That Limit Nutrient Transporter Expression but Lack S1P Receptor Activity and Negative Chronotropic Effects Offer a Novel and Effective Strategy to Kill Cancer Cells in Vivo. *ACS Chem. Biol.* **2016**, *11*, 409–414.

(18) Perryman, M. S.; Tessier, J.; Wiher, T.; O'Donoghue, H.; McCracken, A. N.; Kim, S. M.; Nguyen, D. G.; Simitian, G. S.; Viana, M.; Rafelski, S.; Edinger, A. L.; Hanessian, S. Effects of stereochemistry, saturation, and hydrocarbon chain length on the ability of synthetic constrained azacyclic sphingolipids to trigger nutrient transporter down-regulation, vacuolation, and cell death. *Bioorg. Med. Chem.* **2016**, *24*, 4390–4397.

(19) Garsi, J. B.; Vece, V.; Sernissi, L.; Auger-Morin, C.; Hanessian, S.; McCracken, A. N.; Selwan, E.; Ramirez, C.; Dahal, A.; Romdhane, N. B.; Finicle, B. T.; Edinger, A. L. Design, synthesis and anticancer activity of constrained sphingolipid-phenoxazine/phenothiazine hybrid constructs targeting protein phosphatase 2A. *Bioorg. Med. Chem. Lett.* **2019**, *29*, 2681–2685.

(20) Mayer, S.; Lang, K. Tetrazines in inverse-electron-demand Diels–Alder cycloadditions and their use in biology. *Synthesis* **2017**, *49*, 830–848.

(21) Merkel, M.; Peewasan, K.; Arndt, S.; Ploschik, D.; Wagenknecht, H.-A. Copper-free postsynthetic labeling of nucleic acids by means of bioorthogonal reactions. *ChemBioChem* **2015**, *16*, 1541–1553.

(22) Niederwieser, A.; Späte, A.-K.; Nguyen, L. D.; Jüngst, C.; Reutter, W.; Wittmann, V. Two-color glycan labeling of live cells by a combination of Diels–Alder and click chemistry. *Angew. Chem., Int. Ed.* **2013**, *52*, 4265–4268.

(23) Sečkutě, J.; Devaraj, N. K. Expanding room for tetrazine ligations in the in vivo chemistry toolbox. *Curr. Opin. Chem. Biol.* **2013**, *17*, 761–767.

(24) Erdmann, R. S.; Takakura, H.; Thompson, A. D.; Rivera-Molina, F.; Allgeyer, E. S.; Bewersdorf, J.; Toomre, D.; Schepartz, A. Super-Resolution Imaging of the Golgi in Live Cells with a

Bioorthogonal Ceramide Probe. *Angew. Chem., Int. Ed.* **2014**, *53*, 10242–10246.

(25) Karver, M. R.; Weissleder, R.; Hilderbrand, S. A. Synthesis and evaluation of a series of 1,2,4,5-tetrazines for bioorthogonal conjugation. *Bioconjugate Chem.* **2011**, *22*, 2263–2270.

(26) Fan, X.; Ge, Y.; Lin, F.; Yang, Y.; Zhang, G.; Ngai, W. S. C.; Lin, Z.; Zheng, S.; Wang, J.; Zhao, J.; Li, J.; Chen, P. R. Optimized tetrazine derivatives for rapid bioorthogonal decaging in living cells. *Angew. Chem., Int. Ed.* **2016**, *55*, 14046–14050.

(27) Kubiniok, P.; Finicle, B. T.; Piffaretti, F.; McCracken, A. N.; Perryman, M.; Hanessian, S.; Edinger, A. L.; Thibault, P. Dynamic Phosphoproteomics Uncovers Signaling Pathways Modulated by Anti-oncogenic Sphingolipid Analogs. *Mol. Cell. Proteomics* **2019**, *18*, 408–422.

(28) Sauer, J.; Heldmann, D. K.; Hetzenegger, J.; Krauthan, J.; Sichert, H.; Schuster, J. 1,2,4,5-Tetrazine: synthesis and reactivity in [4 + 2] cycloadditions. *J. Eur. J. Org. Chem.* **1998**, *1998*, 2885–2896.

(29) Sangodkar, J.; Perl, A.; Tohme, R.; Kiselar, J.; Kastrinsky, D. B.; Zaware, N.; Izadmehr, S.; Mazhar, S.; Wiredja, D. D.; O'Connor, C. M.; Hoon, D.; Dhawan, N. S.; Schlatter, D.; Yao, S.; Leonard, D.; Borczuk, A. C.; Gokulrangan, G.; Wang, L.; Svenson, E.; Farrington, C. C.; Yuan, E.; Avelar, R. A.; Stachnik, A.; Smith, B.; Gidwani, V.; Giannini, H. M.; McQuaid, D.; McClinch, K.; Wang, Z.; Levine, A. C.; Sears, A. C.; Chen, E. Y.; Duan, Q.; Datt, M.; Haider, S.; Ma'ayan, A.; DiFeo, A.; Sharma, N.; Galsky, M. D.; Brautigan, D. L.; Ioannou, Y. A.; Xu, W.; Chance, M. R.; Ohlmeyer, M.; Narla, G. Activation of tumor suppressor protein PP2A inhibits KRAS-driven tumor growth. *J. Clin. Invest.* **2017**, *127*, 2081–2090.